VILNIAUS UNIVERSITETAS
FIZIKOS FAKULTETAS
TEORINĖS FIZIKOS KATEDRA

Jonas Narkeliūnas

A NUMERICAL APPROACH TO ESTIMATE THE BALLISTIC COEFFICIENT OF SPACE DEBRIS FROM TLE ORBITAL DATA

Mokslo tiriamasis darbas

(studijų programa – TEORINĖ FIZIKA IR ASTROFIZIKA)

Studentas Jonas Narkeliūnas

Darbo vadovas dr. Jan Stupl

Katedros vedėjas

Vilnius 2016

Contents

Introduction

Low Earth Orbit (LEO) is full of space debris, which consist of spent rocket stages, old satellites and fragments from explosions and collisions. As of 2009, more than 21 000 orbital debris larger than 10 cm are known to exist [1], and while it is hard to track anything smaller than that, the estimated population of particles between 1 and 10 cm in diameter is approximately 500 000, whereas small as 1 cm exceeds 100 million. These objects orbit Earth with huge kinetic energies – speeds usually exceed 7 km/s. The shape of their orbit varies from almost circular to highly elliptical and covers all LEO, a region in space between 160 and 2 000 km above sea level. Unfortunately, LEO is also the place where most of our active satellites are situated[1], as well as, *International Space Station* (ISS) and *Hubble Space Telescope*, whose orbits are around 400 and 550 km above sea level, respectively. This poses a real threat as debris can collide with satellites and deal substantial damage or even destroy them.

Collisions between two or more debris create clouds of smaller debris, which are harder to track and increase overall object density and collision probability. At some point, the debris density could then reach a critical value, which would start a chain reaction and the number of space debris would grow exponentially. This phenomenon was first described by *Kessler* in 1978 and he concluded that it would lead to creation of debris belt, which would vastly complicate satellite operations in LEO. [2].

The debris density is already relatively high, as seen from several necessary *debris avoidance maneuvers* done by Shuttle, before it was discontinued, and ISS [1,3,4]. But not all satellites have a propulsion system to avoid collision, hence different methods need to be applied. One of the proposed collision avoidance concepts is called *LightForce* and it suggests using photon pressure to induce small orbital corrections to deflect debris from colliding [5,6]. This method is very efficient – as seen from theoretical simulations, even few continuous mode 10 kW ground-based lasers, focused by 1.5 m telescopes with adaptive optics, were enough to prevent significant amount of the debris collisions. Simulations were done by propagating all space objects in LEO by 1 year into the future and checking whether the probability of collision was high. For those space objects different ground-based lasers were used to divert them, afterwards collision probabilities were reevaluated. However, the actual accuracy of the LightForce software, which has been developed at NASA Ames Research Center, depends on the veracity of the input parameters, one of which is the object's *ballistic coefficient*. It is a measure of body's ability to overcome air resistance, which has a significant impact on the debris in LEO, and thus it is responsible for the shape of the trajectory of the debris. Having the exact values of the ballistic coefficient would make significantly better collision predictions, unfortunately, we do not know what are the values for most of the objects.

In this research, we were working with part of LightForce code, which estimates the ballis-

[1] Source: *https://www.space-track.org*.

tic coefficient from *ephemerides*[2]. Previously used method gave highly inaccurate values, when compared to known objects, and it needed to be changed. **The goal of this work** was to try out a different method of estimating the ballistic coefficient and to check whether or not it gives noticeable improvements in accuracy. Here we present our new approach and the ideas behind it.

[2] Ephemeris (plural ephemerides) gives the position of astronomical objects as well as space debris in the sky at a given time.

1 Atmospheric Drag

Everything above *Karman line*, 100 km above sea level, is assumed to be outer space, however, atmosphere extends far beyond that point. It extends for at least 10 000 km more [7], although after 600 - 700 km it is not very significant (see Figure 1.1). Nevertheless, besides gravity, the atmospheric drag effect has the most impact on the object's trajectory in LEO and it has to be taken into account when modeling orbits of space objects in LEO. From here everything will eventually fall down to Earth, but the magnitude of the effect depends on many different parameters and we present them in this section.

1.1 Drag Force and Drag Coefficient

An object moving through medium always experiences drag – a resistance force acting in the opposite direction of object's movement. It is a result of three main effects: surface friction, flow interference and form drag. At relatively high velocities and low densities, like in our case, the lateral effect overshadows the first two, so they can be neglected [9]. In this case, the drag force is largely proportional to characteristic area of the object and to the square of its velocity.

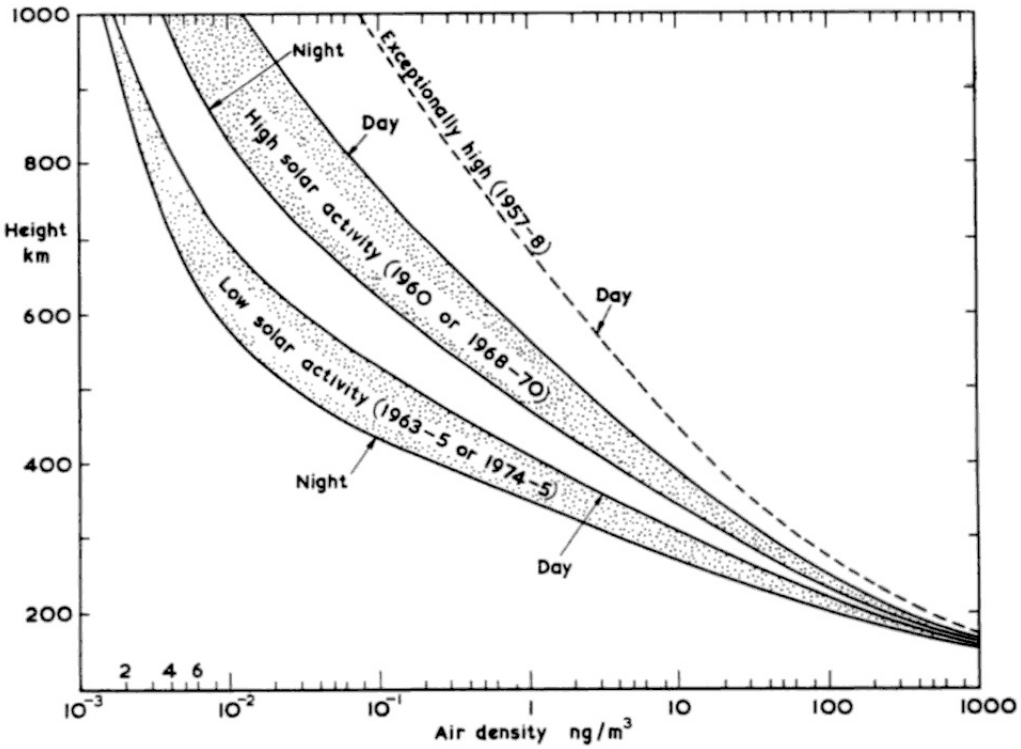

Figure 1.1 Variations of air density with height from 150 to 1000 km for high and low solar activity and diurnal variations (see chapter 1.2) based on COSPAR International Reference Atmosphere (CIRA 1972). Courtesy: King-Hele [8]

Using dimensional analysis from fluid dynamics, we can define drag as follows:

$$F_d = -\frac{1}{2}\rho \left|\mathbf{v_{rel}}^2\right| C_d A, \tag{1.1}$$

where F_d is the drag force; ρ is a density of medium, in our case, the density of air; $\mathbf{v_{rel}}$ is a relative velocity of an object going through medium; and A is a characteristic area of that object. C_d is a drag coefficient; it has no units and depends on the object's surface roughness and shape, as seen from Figure 1.2 – it also depends on the medium's density and the molecular velocity [9]. Nevertheless, the dependence of different parameters for specific conditions are usually too small to take into account, thus it is mostly used as a constant.

When modeling a space object, we usually do not know its shape, because this information is not saved in ephemerides, as seen from chapter 2.1, hence we cannot know what is the exact value of the drag coefficient. Even if we could capture an image of the object's profile and measure the surface area, C_d and A values wouldn't be right, as most of the objects are non-spherical and spinning with respect to their direction of motion, hence one would need multiple pictures of different sides, as well as, to know its angular velocity. A good way to deal with this is to approximate them as spheres and then use drag coefficient of a sphere. The value we use is $C_d = 2.2$, which was popularized by the use of *Jacchia* models for estimating atmospheric density and other parameters of upper layers

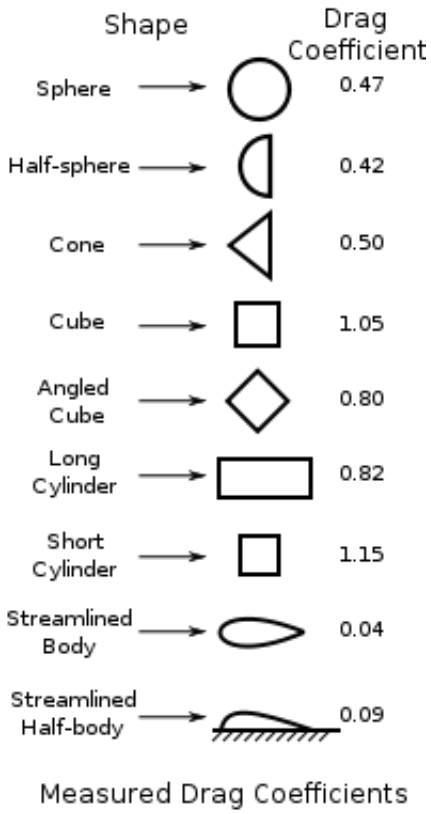

Figure 1.2 Drag coefficient for different shape objects calculated at low velocities [10]

of Earth's atmosphere [11, 12]. Note that this value is different from the one showed in Figure 1.2 as a result of the following assumptions [9]:

- The mean free path of the air molecules is much greater than the size of the satellite.
- The satellite velocity v_0 is much greater than the mean random velocity $\bar{v}$ of the air molecules.
- The mechanisms that deflect the impinging molecules range from elastic to inelastic impact and diffuse evaporation at an effective surface temperature T.

1.2 Atmospheric Density Model

As one can see, the drag force depends on the atmospheric density in different ways, but the density is not constant. Even though we assume that its changes do little effect to the drag coefficient, for the drag force we have to use accurate values, as objects closer to the ground will interact with it a lot more and deorbit quicker than those who are further away; it is easy to see this from the ISS and *Vanguard 1*[3] orbits. While the ISS is the biggest man-made satellite, it has one of the lowest orbits of all artificial satellites and thus it loses 2 or more kilometers of altitude per month, as seen from Figure 1.3. Without frequent orbital corrections it would deorbit within a year. Vanguard 1 is in a higher orbit, with a perigee[4] of 656 km and apogee[5] of 3842 km (as of December 2015), and it is expected to stay in orbit for 240 years [6].

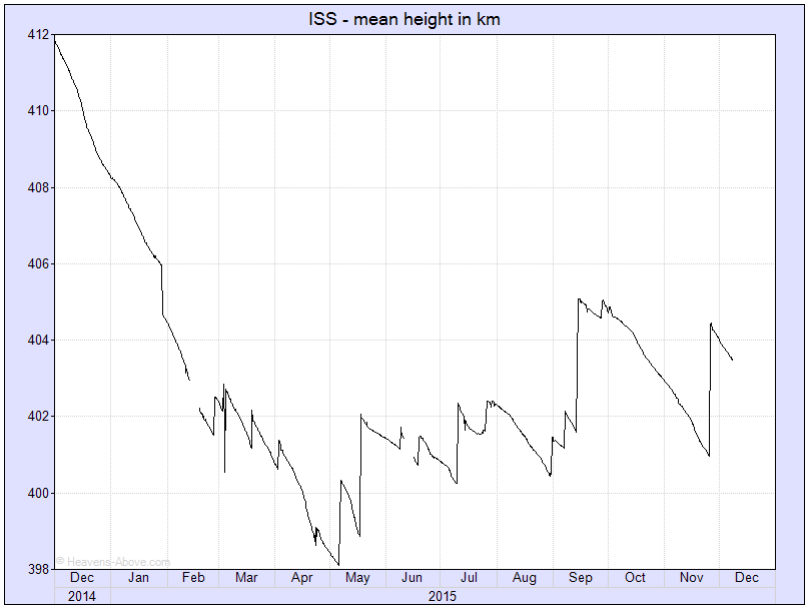

Figure 1.3 Orbital height of the ISS throughout last year. Image source: *www.heavens-above.com/ISSHeight.aspx*

[3] Vanguard 1 is the oldest man made satellite still in orbit, launched in 1958; it was used to obtain geodetic measurements.

[4] A point where celestial body is closest to the Earth.

[5] A point where celestial body is furthest from the Earth.

[6] Retrieved from *http://nssdc.gsfc.nasa.gov/nmc/spacecraftDisplay.do?id=1958-002B.*

The Earth's atmosphere is expanding and contracting in a complex manner all the time, not to mention it is not the same throughout different latitudes and longitudes. Many effects contribute to that and a good atmospheric model should include at least most significant ones, if not all. Below, we list effects that are considered to be most important [13]:

- **Latitudinal variations**: The effect comes from satellite passing over the Earth's equatorial bulge, effectively this changes the actual altitude and, therefore, the density.
- **Diurnal variations**: These variations come from the Earth's rotation and the Sun's irradiation. The day side of the Earth is warmer than the night side, hence the atmosphere expands and bulges over ecliptic plane in the direction of the Sun. Because of the diurnal variations, it's necessary to know latitude, local time, and time of the year.
- **27-day solar-rotation cycle**: This effect arises from Sun's rotation around its axis, which causes fluctuations in the amount of radiation that reaches the Earth.
- **11-year cycle of sunspots**: Solar cycle strongly varies the amount of incoming radiation reaching the Earth. As a result, the Earth's atmosphere heats up different amounts and it expands different amounts throughout the cycle. At the solar maximum the temperature of upper layers of the atmosphere is about two times higher than at solar minimum [14], meaning that the atmosphere has expanded a lot more and debris will be affected more by the drag. In fact, nine times more debris fall to the surface of the Earth during solar maximum than minimum [15]. Furthermore, depending on the altitude, this effect can even cause larger disturbance through solar-radiation pressure than drag [13].
- **Seasonal variations**: These variations come from solar flux fluctuations due to Earth's rotation around the Sun. The Earth's rotational axis is tilted and its orbit is elliptical, thus the Sun's declination and the distance between the Earth and the Sun varies throughout the year.
- **Rotating atmosphere**: The atmosphere is rotating together with the Earth, however, the velocity of lower layer is usually higher because of the friction with the Earth's surface.
- **Winds**: Atmospheric winds and weather create local variations of the temperature and, therefore, the density. Unfortunately, this is difficult to account for, as the weather itself is almost unpredictable because of its sensitivity to changes.
- **Magnetic-storm variations**: Effect comes from fluctuations in the Earth's magnetic field, which affects the amount of charged particles reaching the Earth's atmosphere from the Sun.
- **Irregular short-periodic variations**: Mostly solar flares: sudden increase in solar wind intensity, which also disturbs the Earth's magnetic field.

- **Tides**: Ocean tides and even atmospheric tides as a result of gravitational pull of the Moon can cause small variations in the atmospheric density.

The first model of the Earth's atmosphere above 120 km was created by Nicolet in 1961 [16]. It was an empirical model and used a set of boundary conditions of temperature and partial densities of gases altogether with diffusion theory to get values for higher altitudes. Later it was improved upon several times by Jacchia with empirical data from the new satellites [11, 17, 18]. It was a good model and even today it is still widely used for spacecraft dynamics. However, for more accurate calculations like satellite and space debris orbital simulations, it is better to use a newer model, developed by Mike Picone, Alan Hedin, and Doug Drobof, which is called *NRLMSISE-00* [19]. It is an abbreviation of *US Naval Research Laboratory* and *Mass Spectrometer and Incoherent Scatter Radar* (*00* stands for the year of release), the two primary data sources for development of earlier versions of the model.

NRLMSISE-00 is an empirical model of the Earth's atmosphere from the ground through exosphere. Its outputs are atmospheric density, which we need, as well as temperature and other parameters, while all the necessary input parameters are: year and day time of day; local apparent solar time; geodetic altitude, latitude and longitude; daily and 81 day average of $F_{10.7}$ solar flux[7]; daily geomagnetic index. This model includes most of the effects listed above [19], it is implemented in LightForce code and thus it is the perfect model for our simulations.

[7] 10.7 cm solar radio flux, $F_{10.7}$, is a great indicator of solar activity, as it correlates with sunspots and UV radiation [14], as well as it is easy to measure it on the ground using radio antenna.

2 Numerical Approach

From the previous chapter we learned how the atmospheric drag affects the debris and why it varies in time, but the problem we face that it is very impractical to experimentally measure it without knowing the shape and the size of the debris. However, we can find ratios between mass, drag coefficient and characteristic surface area of debris – the ballistic coefficient, and it can be done numerically from the orbital tracking data. It is explained in this section.

2.1 Input Data

Satellite tracking began in 1957 with the launch of the first man-made satellite into space – *Sputnik*. The first methods for tracking used radio communication and weren't very reliable as they couldn't detect or track objects in space that weren't transmitting internationally agreed frequencies, as some did. At that time, the main reason for satellite tracking was to defend against missile attacks, as a result better methods were conceived. Telescopes with cameras were used instead, as well as radars, although they had their own limitations. Optical tracking systems depended on the weather and only worked during night time, while radar was free from those problems, but it was costly [20]. Nowadays the methods are the same, only the accuracy has increased a bit, albeit still relatively low, and objects as small as 1 cm could now be detected and tracked with ladars [21], which is great for estimating various parameters of the atmosphere, as well as predicting trajectories.

The most popular way for a celestial body's detection and tracking is using a radar system. The detection is done by sending a powerful, yet short, impulse of radio signal into particular part of space and waiting for echoes. Computer analyzes the returned signal and from its strength, shape and time in took to come back it calculates average ephemeris for that object [22]. Tracking, on the other hand, uses *a priori* knowledge where the object is going to be at specific time, so the radar is prepared by pointing to that part of the sky. After detection, it then tracks that object to get new orbital data, which is then saved as one data set. But there is only a finite number of radar sensor sites around the world, and they have a narrow view of the sky, and limited capabilities, meaning that some space object aren't in view all the time. Furthermore, they might not be in a good view or tracked for couple days, thus measurements are rare – from public database[8] we see that it is about one per two days or less.

The format for storing ephemerides is the same as it was 50 years ago. Back then, a set of orbital elements were written in two lines on a *punch card*[9]; from here came the name *Two-Line Element* (TLE) set, meaning this data encoding format. Given a reference frame and an epoch (a reference time when ephemeris were taken), actually only six orbital elements are needed to unambiguously

[8] *www.celestrak.com/NORAD/elements/*

[9] Punch card is a piece of stiff paper that contained either commands for controlling automated machinery or data for data processing applications. Both commands and data were represented by the presence or absence of holes in predefined positions.

define celestial body's position and motion as a result of body having six degrees of freedom. These elements are as follows:

- **Mean motion,** n: Satellite's average rate of motion over one orbit.
- **Eccentricity,** e: The shape of the orbit. 0 means circles; between 0 and 1 – ellipses; 1 – parabola; over 1 – hyperbola.
- **Inclination,** i: Tilt of the orbit plane relative to equatorial plane.
- **Right ascension of the ascending node,** Ω: The angle in the equatorial plane at which satellite crosses the equator from south to north, measured from Greenwich longitude.
- **Mean anomaly,** M: The angular distance from the perigee which a fictional body would have if it moved in a circular orbit, with constant speed, in the same orbital period (true anomaly) as the actual body in its elliptical orbit.
- **Argument of perigee**, ω: The angle along the orbit between ascending node and perigee measured in the direction of motion.

These angles are showed in Figure 2.1. Here we showed only the most important elements of TLE set, albeit there are few more that help identify the object and its trajectory.

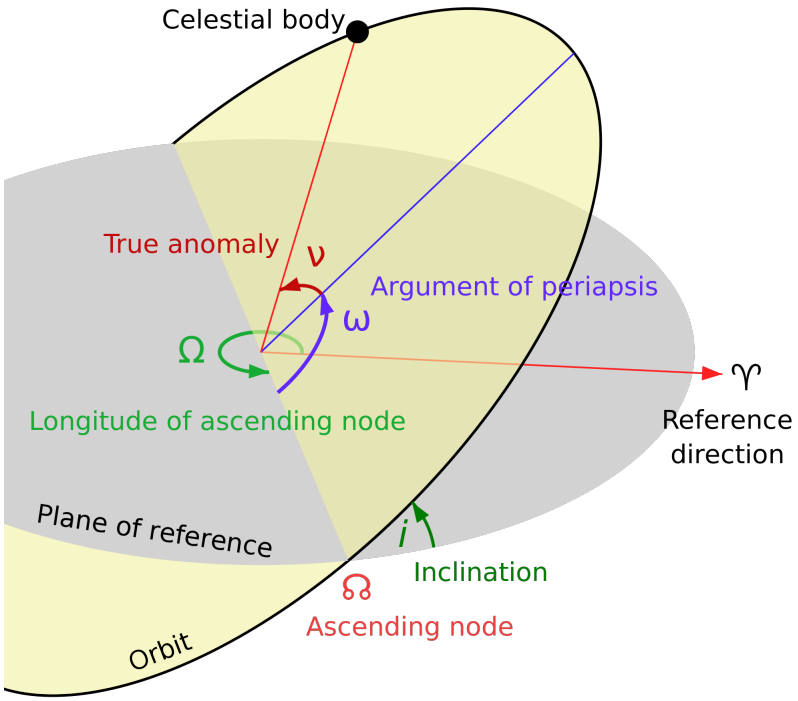

Figure 2.1 Orbital elements that define the position of celestial body. Note that instead of mean anomaly a true anomaly is showed. Image source: *www.wikipedia.com*

These elements are our input data; from them we can calculate the ballistic coefficient, which is used to predict the trajectory of the object. Formula for the ballistic coefficient is derived in the next chapter.

2.2 Ballistic Coefficient

When debris or any other object moves through atmosphere it loses kinetic energy. This means a decrease in total energy and it leads to orbital decay. Orbital decay can easily be seen from decreasing eccentricity and *semi-major axis*[10], but we cannot know how much energy was lost, because we do not know object's mass. Another way to calculate energy loss is from the work done by drag force ((1.1) eq.)– by integrating drag force over the path that debris travels. As mentioned in the previous chapter, for those calculations we need characteristic area and drag coefficient, however, we do not know them either. Fortunately, these two energies are almost the same and, by neglecting the energy fluctuations induced by gravitational field perturbations, we can have an equality:

$$\int_{r_0}^{r} \frac{1}{2}\rho C_d A |\mathbf{v_{rel}}| \left(\mathbf{v_{rel}} \cdot \mathbf{dr'}\right) \simeq \frac{\mu m}{r} - \frac{\mu m}{r_0} + \frac{m v_0^2}{2} - \frac{m v^2}{2}. \tag{2.1}$$

Here μ is the gravitational constant times the Earth's mass; r is the distance from the center of mass and v is the object's velocity relative to the Earth's surface. The left-hand side was already introduced in previous section. Note that when we are calculating relative velocity to Earth's atmosphere, $\mathbf{v_{rel}}$, we are assuming atmosphere rotating with Earth with angular velocity $\omega_\oplus$without winds as that would be impossible to predict. It is expressed with the following equation:

$$\mathbf{v_{rel}} = \mathbf{v} - \omega_\oplus \times \mathbf{r}. \tag{2.2}$$

In (2.1) eq., everything but the mass, characteristic area and drag coefficient, can be calculated or is known from the tracking data. However, the unknowns actually give us the ballistic coefficient

$$B = \frac{m}{C_d A}, \tag{2.3}$$

whose estimation is the main goal of this work. Thus from (2.1) formula we can derive an equation for estimating the ballistic coefficient, and it is as follows:

$$B = \frac{m}{C_d A} \simeq \frac{\int_{t_0}^{t} \rho |\mathbf{v_{rel}}| \left(\mathbf{v_{rel}} \cdot \mathbf{v}\right) dt'}{2\mu\left(\frac{1}{a(t)} - \frac{1}{a(t_0)}\right)} \approx \frac{\sum_{i=1}^{N} \rho |\mathbf{v_{rel}}| \left(\mathbf{v_{rel}} \cdot \mathbf{v}\right) \Delta t}{2\mu\left(\frac{1}{a(t)} - \frac{1}{a(t_0)}\right)} \tag{2.4}$$

In the numerator we changed integration over the distance to integration over the time, hence the

[10]Semi-major axis is a popular unit in the field of astrodynamics. It is defined as half the distance of the longest principal axis of an elliptical orbit. For circular orbits it coincides with radius.

object's velocity relative to the atmosphere is now multiplied by velocity. For numerical approach we also changed integration with summation, thus we introduced Δt, which is an arbitrary size of time step, and $N = \frac{t-t_0}{\Delta t}$. While in the denominator we expressed total energy per mass unit as a function of semi-major axis using this equation: $a = \left(\frac{2}{r} - \frac{v^2}{\mu}\right)^{-1}$. This was done as it is more convenient to calculate ballistic coefficient from TLE set data. Hence now we have a formula for the ballistic coefficient estimation and we can solve it numerically.

2.3 Integration Using SGP4

Orbital elements define space object's orbit and motion, but for our calculations they are not easy to use. It is useful to transform them to a different *state vector* – a position vector and a velocity vector, which we can use in the (2.4) equation. The best way to get the state vector is to use *SGP4 propagator* – a simplified general perturbation model, which was purposely designed to work with the TLE set data [23]. As the name implies, this model uses simplified perturbations to model orbit of the space object. Simplifications were done by assuming static atmosphere and including only the biggest perturbations of gravitational field as well as guessing the value of the ballistic coefficient. Also, SGP4 propagator can estimate the object's state vector for any arbitrary point in time, although its predictions are limited by its accuracy, as even small state vector errors start to grow exponentially over time. This is mostly due to it using its own estimate of ballistic coefficient calculated from one TLE set, which, as mentioned previously, is not perfectly accurate.

In the 2.1 chapter, we mentioned that TLE sets are rare – about one TLE per two days, then on average we have around two hundred TLE data sets per one year. It is clearly not enough for an accurate summation in (2.4) eq. as we are describing changes of the velocity and the atmospheric density that are happening in minute scale and not day scale, as showed in Figure 2.2. Nevertheless, in the old method it is done with even less. Even though the approach is different, the idea behind it is very similar to the new method. It calculates semi-major axis decay per orbit from average values of only few TLE sets and using the same averaged values it integrates to find the drag effect for one orbit. From here, similarly like in (2.4) eq., it is possible to estimate the ballistic coefficient. However, using averaged values, especially from small pool of TLE sets, it gives biggest errors of this method.

On the other hand, in the new method we are trying to capture all of those details, thus we need more data points and for this reason we are using SGP4 propagator to generate it. Even though the accuracy of the model degrades exponentially by every day since the epoch [24], we are only using it for short propagations. From Levit *et al* article [25], it is clear that propagating about 2 days is still accurate as errors are less than 1 km for most debris, after that it is best to take have new TLE set from the next epoch. Fortunately, SGP4 can propagate forwards and backwards in time, thus we can have a total difference of 4 days between any two TLE sets without sacrificing accuracy of our calculations.

For a better accuracy of estimating the ballistic coefficient we would need a very small time step Δt, in the orders of seconds, however, these calculations would take extremely long time and that is inconvenient. By experimenting with different values we noticed that it is best to use time step of 1 minute. It means that we have about 100 data points per orbit (LEO satellite's period is around 100 minutes) which is enough to capture the atmospheric density changes throughout different parts of the orbit.

2.4 Fast-Fourier Transformation

The numerical data generated by SGP4 propagator includes a lot of physical phenomena that make the energy and thus the semi-major axis oscillate throughout the orbit and time. This effect can be easily seen in the Figure 2.2 where we plotted debris's semi-major axis over time using SGP4 generated data. Interestingly enough, from the original TLE set data (generated state vector at TLE epoch) it would appear that debris's orbital height is increasing. With more data, even if it is generated by SGP4 propagator, we can capture intrinsic behavior of the semi-major axis and see that original TLE set data is only a snap-shots of that, thus first assumption would have been most likely false. By our guess, the illusion of growing orbit can be created by orbital precession – rotation of the orbit itself, which is not included in the original TLE set data. By plotting yet another object's semi-major axis values over time in top Figure 2.3 we can actually see oscillations of semi-major axis over time scale that is not explained by any other phenomena, thus supporting this idea. As shown in bottom Figure 2.3, if the celestial body is observed from the same spot on the Earth, like using the same radar or telescope site, it will detect the body at different sections of its the orbit. This can be supported by the fact that from the semi-major axis plot it is visible that TLE sets are almost equally spaced, meaning that measurements are periodical and it is most likely to be true if the same observatory is taking ephemerides of that debris.

Looking into the lower Figure 2.2, we can also see that oscillations are so big that they actually hide any changes that happen to the semi-major axis due to the drag effect. Up until now these oscillations were necessary for the accurate orbit determination but now they are overshadowing the evaluation of the semi-major axis decay. Using this data would lead to the negative ballistic coefficient and our estimation would be most likely wrong. Although sometimes negative values are meaningful, as some satellites have propulsion systems and can do orbital maneuvers, like the ISS, but most of them are debris or passive satellites and should naturally decay. Actually, we expect to find more than 95 % of celestial bodies to have a positive decay values [1] as only few percent are working satellites and out of them only few have propulsion, but first we need additional step – filter the data.

From all the phenomena that are affecting semi-major axis we can only include those who cause drag fluctuations – the rest we must remove. This is a necessary step because otherwise (2.4) eq. becomes invalid. By writing that equation, we neglected gravitational perturbations, so

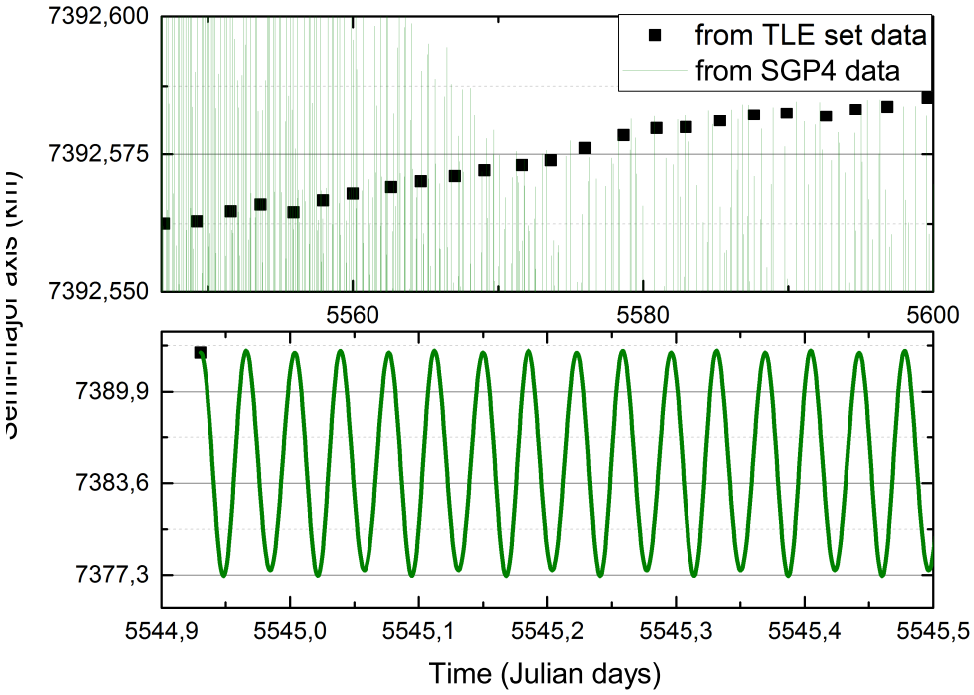

Figure 2.2 Semi-major axis over time. Black squares are semi-major axis at TLE epoch, green line are generated by propagating from epoch. All data generated using SGP4 propagator. Satellite's catalog number: NORAD 299

that semi-major axis decay could be written as equal to energy lost due to drag. Thus we have the same thing here, we must remove gravitational perturbations, which are caused by a *non-spherical gravity* (the Earth has a non-uniform mass distribution) and a *three-body gravity* (Moon, Earth and Sun) [13, 23]. Lateral effect will cause long-periodic and short-periodic variations of the semi-major axis, while the non-spherical gravity will only cause the short-periodic variations. By short-periodic, we mean oscillations on the same scale as celestial body's orbital period; while the long-periodic variations are above tens of days. Knowing this, we can remove these effects by applying *Fourier transformation* to SGP4 propagator generated data [26]. However, to accurately do it, we first need to remove non-periodic energy decay, which is caused by all of the phenomena. This can be easily done by applying *simple linear regression* to find line fit of the data: slope k and intercept b:

$$k = \frac{\bar{xy} - \bar{x}\bar{y}}{\bar{x^2} - \bar{x}^2};$$
$$b = \bar{y} - k\bar{x}, \tag{2.5}$$

and subtracting the fitted line from the data. In this case, we are left with pure oscillations with no decay and algorithm for fast Fourier transformation (FFT) can be used, although here we will not

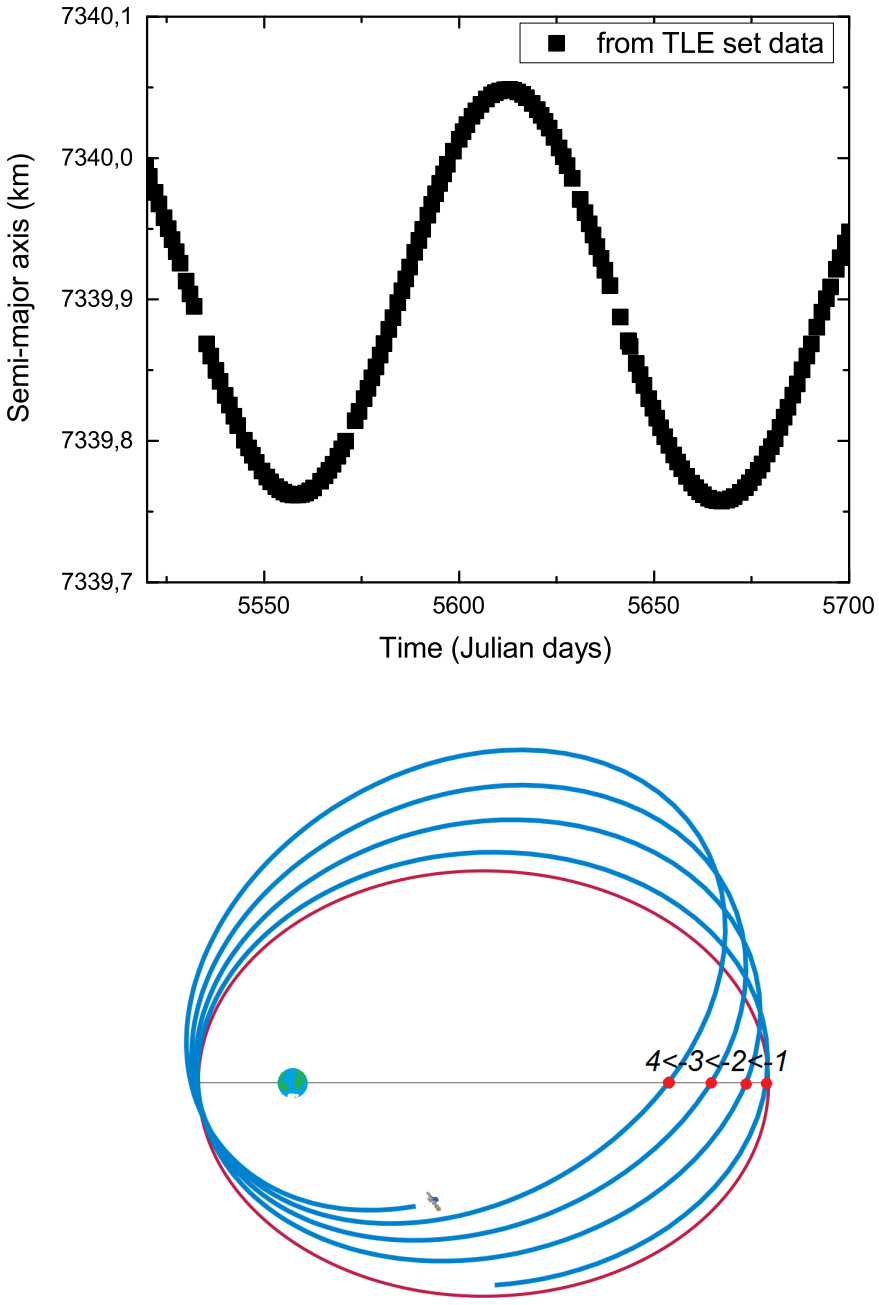

Figure 2.3 Top: The semi-major axis over time of the object NORAD 7646. Bottom: Satellite's orbital precession around The Earth. For an observer standing still on one point of the Earth it appears that satellite's orbit declines

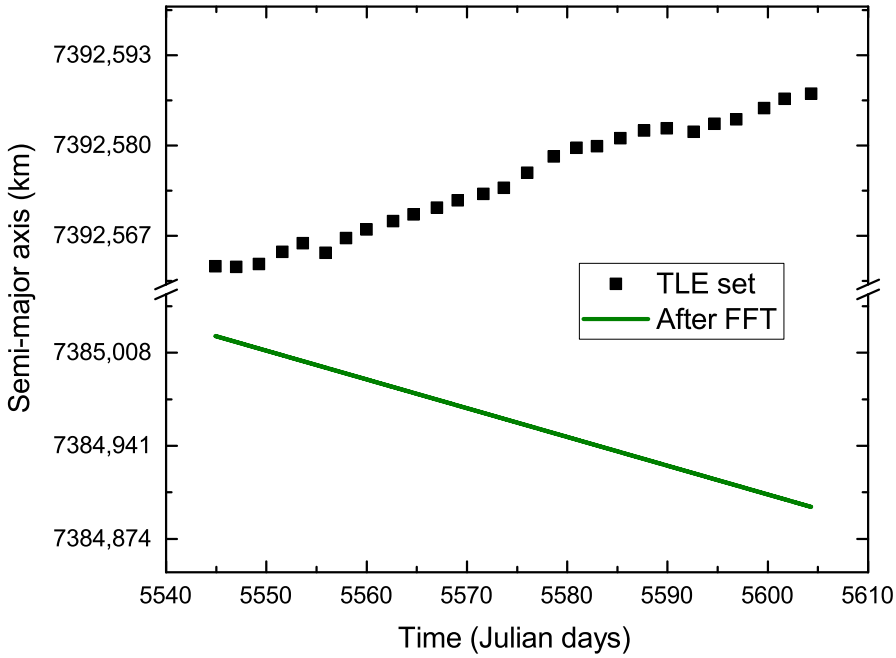

Figure 2.4 Semi-major axis over time before and after fast Fourier transformation. Black squares are from TLE set data, while green line was found after FFT applied to SGP4 generated data

go into further details.

FFT transforms data from time domain to frequency domain. By choosing which frequencies we want to include, we can control what effects we exclude. As most of the unwanted effects are in the high frequency range (short-periodic) we chose to use *low pass filter*[11]. In our calculations the cut-off frequency is one oscillation per 45 days – amplitude is set to zero for anything faster than that. This is an arbitrary value, however, it was chosen to be big enough to exclude gravitational perturbations of the Moon's rotation around the Earth, but low enough to include seasonal effects of solar radiation. Hence, by having TLE set data of about 200 days, we are left with only few lowest frequencies and almost linear relation of the semi-major axis over time. Unfortunately, for some objects with too few TLE sets we do have perfectly linear relation, as seen in Figure 2.4. Nevertheless it is still better than leaving it unchanged, as now we can clearly see that object's orbit is decaying, which would have been probably missed by previous method.

In the next section we present results of the new approach and compare them with previous method, as well as with some known values of the ballistic coefficient.

[11] A low-pass filter passes signals with a frequency lower than a certain cutoff frequency and attenuates signals with frequencies higher than the cutoff frequency.

3 Results

For our calculations, we only used TLE set data[12] from the year 2015. Part of the data, from January 1st till August 15th, was used for the ballistic coefficient calculation, while the rest, from August 16th to September 15th, was used to analyze the accuracy of the estimated values. In general, we would want to extend the first period as we want to have as many TLE sets as possible for a more accurate estimation, however, this work was done by focusing on implementing the new approach and checking whether or not it works better than previously used method, and for this reason we used the same data as was used in previous calculations.

Furthermore, at this stage software is incapable of allocating memory for more than 200 TLE sets, albeit from Figure 3.1 we see that most objects have fewer number of TLE sets. Actually, most objects have as few as 14 TLE sets, while average value is 75. Note that these results came after doing initial data filtration, which removed outliers (data points that are more than 2σ away from the mean) and TLE sets that are too much separated in time to have a good estimation by SGP4 propagator, as explained in chapter 2.3. These steps reduced the total number of available TLE sets substantially, leading to distribution we see in Figure 3.1.

Whenever we estimate the ballistic coefficient for the whole catalog of tracked objects (>13 000) it takes two whole days, plus an additional day if we want a *least squares fitting*[13] on top of that. The least squares fitting algorithm was already implemented in the code and it usually improves the

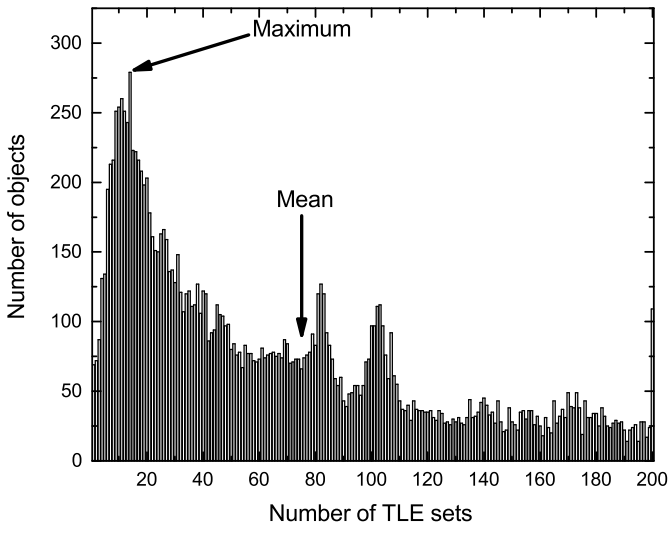

Figure 3.1 Number of objects with different number of TLE sets. Data collected from the period January 1st to August 15th of 2015

[12] All data was downloaded from *www.space-track.org*.

[13] Least squares fit is a statistical method that minimizes the sum of squares of the errors made in the results of every single equation.

accuracy of the ballistic coefficient. It uses a high precision propagator to propagate the trajectory, while TLE snapshots are used as virtual observations for the fit. Nevertheless, the least squares fit uses our estimated values of the ballistic coefficient as its initial guesses, even though it is very sensitive to local minimum, meaning that after this step values are still quite similar. As this step specifically is unrelated to this work, we only did it to compare the new results with the old ones and they were calculated by the previous approach plus the least squares fitting. Unfortunately, data analysis is difficult, as we don't know anything about the true values of the ballistic coefficient of the debris and most satellites. We can only compare our results with some (not all) that we know and whose shape is simple, like sphere, cylinder or cube, as well their mass and size is known. In this case, we can manually calculate the ballistic coefficient using the same formula as in (2.3) eq., where $C_d = 2.2$ is the drag coefficient of the sphere. This data is showed in Table 3.1.

By looking at the Table 3.1, we can see that in many cases the new approach is significantly better than the old one. Albeit it is still underestimating the ballistic coefficient by about one order of magnitude. Most likely this could happen, if the atmospheric drag is weaker than it should have been, which could have been caused by partly underrated atmospheric density. By plotting accuracy of the ballistic coefficient (a ratio between the estimated value and real value) against object's inclination, as it is done in Figure 3.2, we can actually see a correlation between the two. One can see that for all space objects, whose orbits are equatorial (orbital plane is parallel to equator), the accuracy of the ballistic coefficient is significantly worse than for the objects, whose orbits are inclined or even perpendicular to equatorial plane. This relationship between accuracy and inclination can be explained by underestimating bulging of the Earth's atmosphere. Albeit NRLMSISE-00 includes effects like that, SGP4 doesn't – it uses simple model of static atmosphere, as mentioned in chapter 2.3. In the previous approach SGP4 propagator isn't used in the same manner as in the new method, thus there is no reason for it to exhibit similar behavior throughout different inclinations and should show no correlation – that is what we see in Figure 3.2.

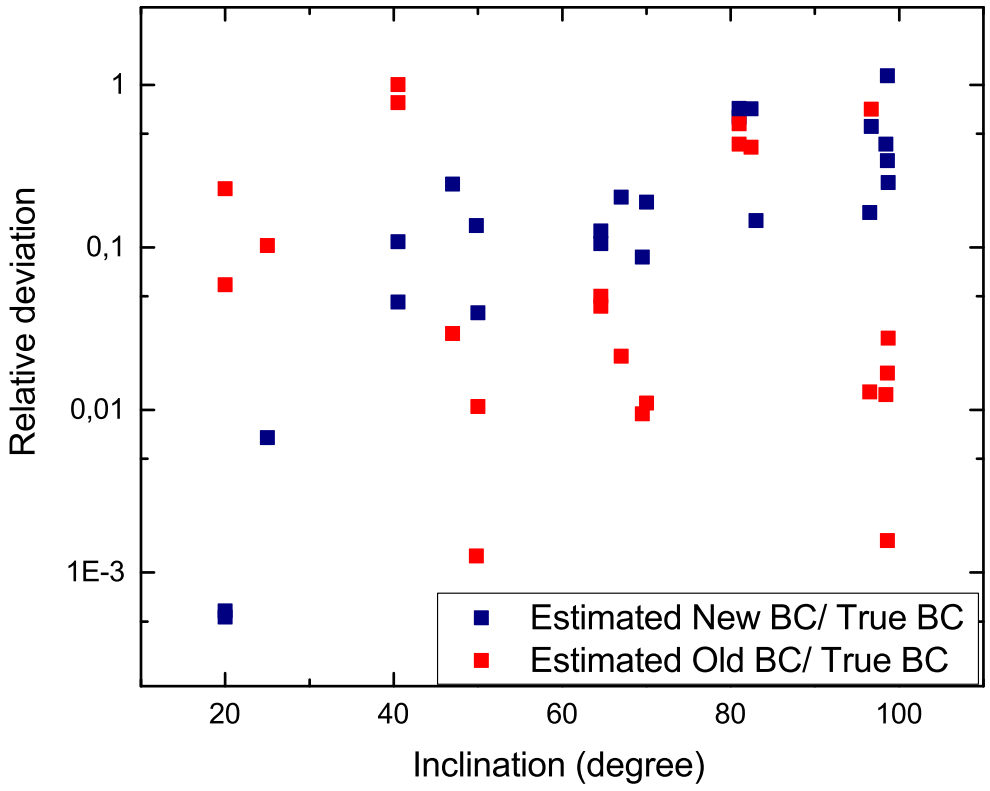

Figure 3.2 Accuracy of the ballistic coefficient of the old (red) and the new (navy blue) methods plotted against inclination. Accuracy is measured as a ratio between estimated value and "true" value

Table 3.1 Comparison of the true ballistic coefficient versus estimated value for satellites with simple shapes

Name	NORAD ID	Mass (kg)	Dimensions (m)/Shape	Inclination	Apogee/Perigee (km)	Eccentricity	B_{true}	$\boldsymbol{B_{\text{est.}}^{\text{new}}}$	$B_{est.}^{old}$
STARLLETE	7646	47.3	⌀0.24/sphere	49.8	1107/805	0.15679	475	**64.7**	0.60
AJISAI	16908	685	⌀2.15/sphere	50.0	1503/1485	0.00602	85.8	**3.41**	0.90
STELLA	22824	48.0	⌀0.24/sphere	98.6	805/797	0.00499	482	**165**	0.76
LARES	38077	387	⌀0.36/sphere	69.5	1456/1445	0.00379	1728	**151**	16.4
DANDE	39267	38.0	⌀0.46/sphere	81.0	1390/328	0.61816	104	**74.6**	59.9
KIKU 1 (ETS 1)	8197	85.0	⌀0.9/spherical	47.0	1109/981	0.06124	60.7	**14.9**	1.79
NADEZHDA 2	20508	870	⌀2×3.5/cylindrical	83.0	1023/960	0.03177	126	**18.4**	-
SCD 1	22490	115	⌀1×1/cylindrical	25.0	782/720	0.01664	66.6	**0.45**	6.85
FORTE	24920	41.0	⌀0.8×2/cylindrical	70.0	825/798	0.01664	37.1	**7.05**	0.41
ORSTED	25635	50.0	0.34×0.45 × 8.72/rectangular	96.5	833/632	0.13720	148	**24.4**	1.91
PCSAT	26931	10.0	0.25^3/cube	67.0	795/787	0.00506	37.3	**7.60**	0.80
FEDSAT	27598	50	0.58^3/cube	98.4	811/797	0.00871	69.3	**29.9**	0.86
LATINSAT B	27606	12	0.25^3/cube	64.6	727/598	0.09736	89.6	**11.3**	4.48
SAUDISAT 1C	27607	10	0.23^3/cube	64.6	709/596	0.08659	88.2	**9.29**	3.84
AAU CUBESAT	27846	1	0.1^3/cube	98.7	833/818	0.00909	46.7	**11.7**	1.29
SEEDS	32791	1	0.1^3/cube	96.7	617/597	0.01647	46.7	**25.9**	33.1
VESSELSAT 1	37840	29.0	0.3^3/cube	20.0	874/854	0.01157	150	**0.081**	34.4
SRMSAT	37841	10.4	0.28^3/cube	20.0	875/856	0.01098	61.9	**0.036**	3.66
TUGSAT-1	39091	7.00	0.2^3/cube	98.6	790/776	0.00894	40.8	**46.4**	0.69
CASSIOPE	39265	500	⌀1.8×1.25/cylindrical	81.0	1358/329	0.60996	89.3	**56.4**	38.6
DRAGONSAT	39383	1.00	0.1^3/cube	40.5	402/402	0	46.7	**2.30**	46.8
COOPER	39395	1.00	0.1^3/cube	40.5	336/319	0.02595	46.7	**2.16**	36.3
AIST 1	39492	39.0	0.47 × 0.56 × 0.48/rectangular	82.4	628/599	0.02363	72.8	**51.8**	30.2

Another way of checking the accuracy of our method is by launching body propagator, implemented in Lightforce software. By putting calculated values of the ballistic coefficient as a new input, we can see how much object's position deviates from the TLE set data that was not used for the estimation of the ballistic coefficient. Furthermore, we can do the same with values from the old approach, hence we can compare the accuracy of both methods against each other and against experimental measurements. Here, we chose to propagate only 4 *geodetic* satellites[14], as they are spherical in shape and in theory should show best results. Results are plotted in Figure 3.3.

It is easy to see that in all examples the new method performs better than the old one. Positional errors of the new method are significantly smaller, sometimes by two orders of magnitude smaller, like in graphs of AJISAI and STELLA. Here we can see that even after two months the positional errors are relatively small and not growing exponentially. By looking at the graph of AJISAI satellite, we can even see that the expected position of the satellite was on the other side of the Earth than it really was after 25 days of propagation with the old approach. Oscillations visible in the same graph are actually caused by our imaginary satellite going around the Earth and catching up with real one. Only in the graph of satellite DANDE we see similarly bad performance, albeit the estimated values of the ballistic coefficient for DANDE are closest to the real value out of all four satellites. This could be caused by highly elliptical orbit, as out of all four it has the highest eccentricity. STARLETTE has the second biggest value of eccentricity and the positional errors in time exhibit similar behavior. Thus highly elliptical orbits might pose another problem for the accuracy of calculations.

Lastly, when we looked throughout the list of all tracked space objects and their estimated values of the ballistic coefficient, we calculated the percentage of the objects with negative values. We found that there is only 4.57 of the objects with such values. In chapter 2.4, we emphasized that less than 5% of tracked objects are active satellites, although few of them do have propulsion system, we can see that the new method gives absolutely wrong values for only couple of percents of tracked objects. On the other hand, the old approach gives almost one fourth of the time (26.04%) negative values, which is at least 5 times worse, when compared to the new approach.

[14]The geodetic group of satellites are inactive targets for satellite laser ranging that are used for positioning, gravitational field modeling and atmospheric modeling.

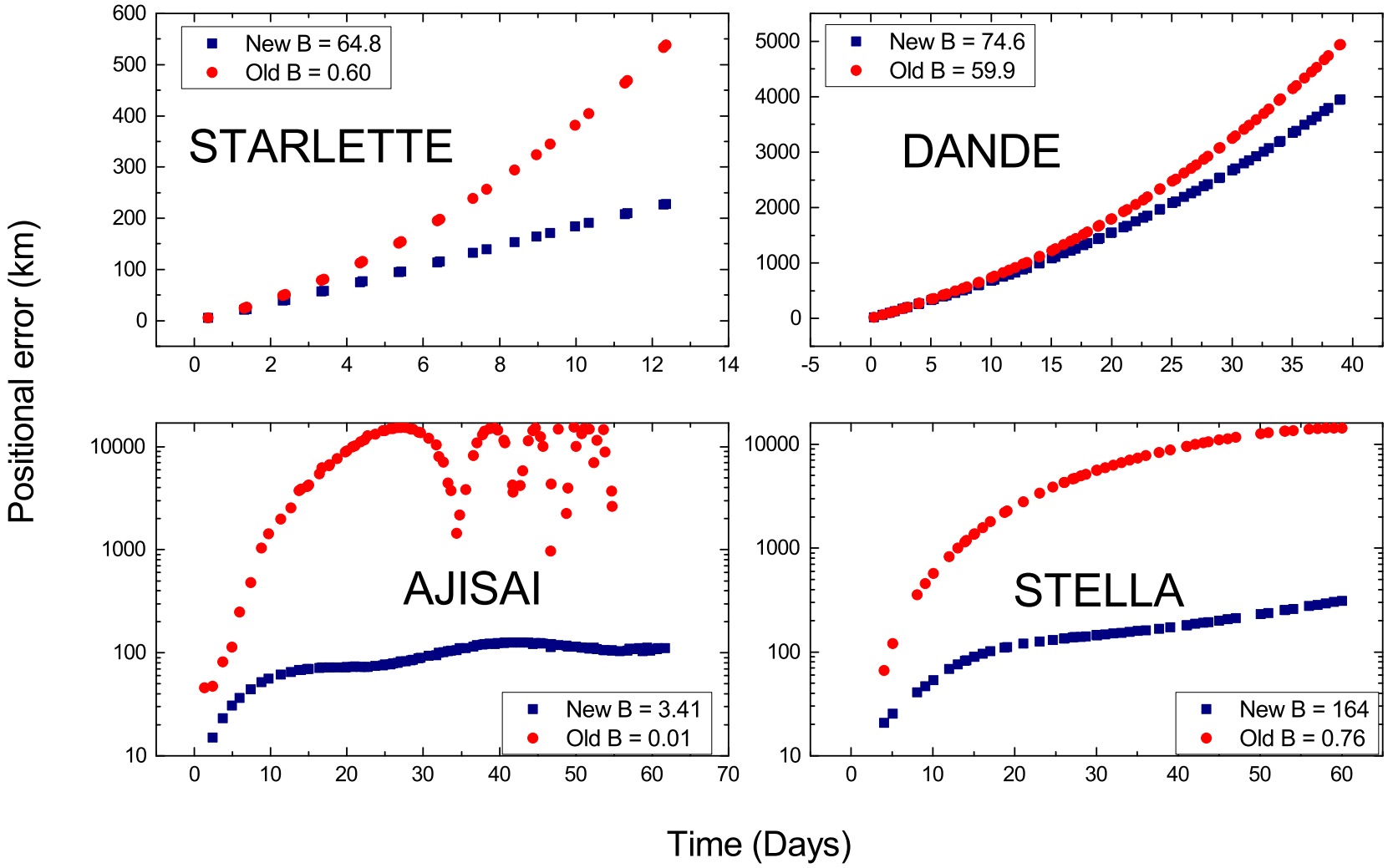

Figure 3.3 Positional errors calculated using the new approach (navy blue) and the old approach (red). *x*-axis are days of propagation. Note different time scales

Conclusion

- The new approach implemented in the Lightforce code gives significantly better results when compared to the old version of the code. The new estimated values are mostly within one order of magnitude away from the real values, usually being underestimated, while the older ones were mostly two or more orders of magnitude away.
- We showed that the accuracy of the new approach is inclination dependent while this is not visible in the previous method. We suspect that errors arise from SGP4 model underestimating the Earth's atmospheric density at equatorial plane, which is consistent with the results from the geodetic satellites.
- When propagating object's trajectory with new values, we see a lot smaller positional errors from previously used method. Positional errors are two orders of magnitude smaller than they were before, thus Lightforce simulations can now be used to predict real collision threats within moderate accuracy.

References

[1] *The Threat of Orbital Debris and Protecting NASA Space Assets from Satellite Collisions*, Technical report, National Aeronautics and Space Administration (2009).

[2] D. J. Kessler, B. G. Cour-Palais, Collision frequency of artificial satellites: The creation of a debris belt, Journal of Geophysical Research: Space Physics (1978–2012) **83**(A6), 2637–2646 (1978).

[3] K. T. Alfriend, M. R. Akella, J. Frisbee, J. L. Foster, D.-J. Lee, M. Wilkins, Probability of collision error analysis, Space Debris **1**(1), 21–35 (1999).

[4] J. L. Foster Jr, The analytic basis for debris avoidance operations for the international space station, in *Space Debris* (2001), volume 473, 441–445.

[5] J. Stupl, J. Mason, W. Marshall, C. Levit, C. Smith, S. Olivier, A. Pertica, W. De Vries, LightForce: Orbital collision avoidance using ground-based laser induced photon pressure, in C. Phipps (ed.), *American Institute of Physics Conference Series* (2012), volume 1464 of *American Institute of Physics Conference Series*, 481–491.

[6] J. Stupl, N. Faber, C. Foster, F. Y. Yang, B. Nelson, J. Aziz, A. Nuttall, C. Henze, C. Levit, Lightforce photon-pressure collision avoidance: Updated efficiency analysis utilizing a highly parallel simulation approach, in *Advanced Maui Optical and Space Surveillance Technologies Conference* (2014), volume 1, 9.

[7] S. Bauer, H. Lammer, *Planetary Aeronomy. Atmosphere Environments in planetary Systems*, 1610-1677 (Springer-Verlag Berlin Heidelberg, 2004), 1 edition.

[8] D. G. King-Hele, *Satellite orbits in an atmosphere: theory and application* (Springer Science & Business Media, 1987).

[9] R. Stirton, The upper atmosphere and satellite drag, Smithsonian contributions to astrophysics **5**(2) (1960).

[10] L. Clancy, *Aerodynamics*, Pitman Aeronautical Engineering Series (Wiley, 1975).

[11] L. G. Jacchia, Static diffusion models of the upper atmosphere with empirical temperature profiles, Smithsonian Contributions to Astrophysics **8**, 215 (1965).

[12] B. R. Bowman, K. Moe, Drag coefficient variability at 175–500 km from the orbit decay analyses of spheres, Advances in the Astronautical Sciences **123.1**, 117–136. (2005).

[13] D. A. Vallado, *Fundamentals of Astrodynamics and Applications* (Microcosm Press, 2013), fourth edition.

[14] K. F. Tapping, The 10.7 cm solar radio flux (f10.7), Space Weather **11**(7), 394–406 (2013).

[15] N. Johnson, Space debris issues, Audio File, @0:05:50-0:07:40. The Space Show (2011).

[16] M. Nicolet, Structure of the thermosphere, Planetary and Space Science **5**(1), 1–32 (1961).

[17] L. G. Jacchia, Revised static models of the thermosphere and exosphere with empirical temperature profiles, Smithsonian Astrophysical Observatory Special Report (332) (1971).

[18] L. G. Jacchia, Thermospheric temperature, density, and composition: new models, SAO special report **375** (1977).

[19] J. M. Picone, A. E. Hedin, D. P. Drob, A. C. Aikin, Nrlmsise-00 empirical model of the atmosphere: Statistical comparisons and scientific issues, Journal of Geophysical Research: Space Physics **107**(A12), SIA 15–1–SIA 15–16, 1468 (2002).

[20] D. G. King-Hele, Review of tracking methods, Philosophical Transactions of the Royal Society of London. Series A, Mathematical and Physical Sciences **262**(1124), 5–13 (1967).

[21] B. Greene, Y. Gao, C. Moore, Laser tracking of space debris, in *13th International Workshop on Laser Ranging Instrumentation, Washington DC* (2002).

[22] D. Mehrholz, L. Leushacke, W. Flury, R. Jehn, H. Klinkrad, M. Landgraf, Detecting, tracking and imaging space debris, ESA Bulletin (0376-4265) (109), 128–134 (2002).

[23] F. R. Hoots, R. L. Roehrich, Spacetrack report no. 3, Colorado Springs CO: Air Force Aerospace Defence Command 1–3 (1980).

[24] D. A. Vallado, P. Crawford, R. Hujsak, T. Kelso, Revisiting spacetrack report no. 3, AIAA **6753**, 2006 (2006).

[25] C. Levit, W. Marshall, Improved orbit predictions using two-line elements, Advances in Space Research **47**(7), 1107 – 1115 (2011).

[26] J. W. Cooley, J. W. Tukey, An algorithm for the machine calculation of complex fourier series, Mathematics of computation **19**(90), 297–301 (1965).

Jonas Narkeliūnas

SKAITMENINIŲ METODŲ TAIKYMAS KOSMINIŲ ŠIUKŠLIŲ BALISTINIO KOEFICIENTO APSKAIČIAVIMUI, PASITELKIANT TLE ORBITINIUS DUOMENIS

Santrauka

Kosminės šiukšlės yra auganti bėda, su kuria tenka susidurti bet kuriam bandančiam sėkmingai vystyti tyrimus žemutinėje Žemės orbitoje. Kosminės šiukšlės yra sudarytos iš panaudotų raketinių variklių, nebeveikiančių palydovų ir skeveldrų, pažertų po sprogimų ir susidūrimų tarp tų pačių nuolaužų, ir jos skrieja aplink Žemę su milžiniškomis kinetinėmis energijomis. Net mažiausia šiukšlė/skeveldra lekianti 7 km/s greičiu gali perskrosti saulės elementus, o vos 1 cm dydžio gali net pažeisti korpusą raketos gabenančios žmones ar krovinius. Didžiausią grėsmę šiuo metu jos kelią Tarptautinei Kosminiai Stočiai (TKS), kurioje nuolat yra grupė žmonių – būtent dėl šiukšlių TKS tenka atlikinėti įvairius manevrus, kad išvengtų susidūrimo rizikos. Tačiau nevisi dirbtiniai palydovai turi raketinius variklius, tad jie neturi galimybės išvengti susidūrimo. Jam įvykus, palydovas gali būti sunaikintas ir tapti nauju kosminių šiukšlių debesiu, kuris atsitiktinai gali pataikyti į dar kitus palydovus ar tas pačias kosmines šiukšles. Pasiekus tam tikrą kritinį tankį šis procesas pradės dažnėti eksponentiškai ir kosminių šiukšlių skaičius sparčiai išaugs. Tuomet žemutinė Žemės orbita bus tankiai užpildyta kosminėmis šiukšlėmis ir nebus galima vykdyti jokios veiklos, tad akivaizdu, kad kosminės šiukšlės kelią didelį pavojų tiek dabartiniams palydovams, tiek ateityje planuojamoms kosminėms misijoms.

Jau šiuo metu kosminių šiukšlių koncentraciją yra didelė ir, jei nieko nebus imtasi, o palydovų bus keliamą į orbitą vis daugiau, tai šis scenarijus greitai išsipildys. Dėl šios priežasties yra vystomos įvairios koncepcijos kosminių šiukšlių susidūrimų mažinimui ir jų pašalinimui. Viena tokia koncepcija vadinasi LightForce – tai yra simuliacijų paketas, skirtas sumodeliuoti ir įvertinti ar galima išvengti kosminių šiukšlių susidūrimų naudojant antžeminius lazerius [5]. LightForce prognozuoja, kuriuos kosminės šiukšlės susidurs, ir prieš tam įvykstant, truputį pakeičia jų greičius pasitelkiant lazerio šviesos pluoštus taip, kad jos saugiai prasilenktų. Teoriškai jau yra įrodyta, kad šitas metodas yra veiksmingas, tačiau prieš pritaikant programą praktiniams bandymams reikia pagerinti jos prognozių tikslumą. Pastarosios labai priklauso nuo balistinio koeficiento vertės, kuri nusako, kaip smarkiai ar silpnai objekto trajektoriją paveiks oro pasipriešinimas. Tačiau balistinis koeficientas kosminėms šiukšlėms yra nežinomas, kadangi jis priklauso nuo masės ir charakteringo ploto, taip pat ir nuo pasipriešinimo koeficiento, priklausančio nuo objekto formos, o šių duomenų tiesiogiai išmatuoti mes negalime. Tokiu atveju balistinis koeficientas yra ieškomas netiesiogiai iš orbtinių duomenų, pasitelkiant skaitmeninius metodus. Vis dėlto ankstesnėje programos versijoje naudoti skaitmeniniai metodai davė pakankamai netikslias balistinio koeficiento vertes, o tai reiškia, kad objektai galėjo būti toli nuo prognozuotų pozicijų, tad netiksliai buvo prognozuojami

ir susidūrimai. **Šio darbo tikslas** buvo pagerinti balistinio koeficiento apskaičiavimo metodą.

Šiame darbe išvedėme naują formulę balistinio koeficiento apskaičiavimui, kurią galima skaitmeniškai išspręsti iš turimų orbitinių duomenų. Siekiant geresnio tikslumo taip pat pritaikėme įvairius duomenų tvarkymo ir papildomų duomenų generavimo metodus. Gauti rezultatai parodė, kad kiekybiškai naujasis metodas duoda net pora eilių tikslesnes vertes lyginant su ankstesniu metodu ir tikromis balistinio koeficiento vertėmis (tikros vertės gali būti apskaičiuojamos žinomos formos, dydžio ir masės palydovams). Taip pat naudojant naujas vertes gaunamos žymiai geresnės prognozės palydovo trajektorijai, tad ir susidūrimai gali būti geriau įvertinti negu anksčiau. Taigi akivaizdžiai sugebėjome pagerinti programos veikimą – simuliacijų tikslumą.